Detection and analysis of non-conformities in S355JR non-alloy structural steel

Kozina, Franjo; Zovko Brodarac, Zdenka; Voloder, Luka; Grgić, Ivan

SVEUČILIŠTE U ZAGREBU
METALURŠKI FAKULTET
UNIVERSITY OF ZAGREB
FACULTY OF METALLURGY

dabar
DIGITALNI AKADEMSKI ARHIVI I REPOZITORIJI

Detection and analysis of non-conformities in S355JR non-alloy structural steel

Franjo Kozina[1], Zdenka Zovko Brodarac[1], Luka Voloder[2] and Ivan Grgić[3]

1) University of Zagreb Faculty of Metallurgy, Aleja narodnih heroja 3, 44000 Sisak, Croatia

2) Delta MM Steelix d.o.o., Božidara Adžije 2A 44000, Sisak, Croatia

3) TPK-ZAVOD d.o.o. Zavod za energetsku i procesnu opremu, Slavonska avenija 20, 10000 Zagreb, Croatia

Corresponding author: fkozin@simet.unizg.hr

Type of paper

Abstract: Although construction materials are considered the most predictable components of a construction project, design and material challenges represent a major cause of productivity loss. The occurrence of non-conformities is a consequence of the very difficult quality assurance under industrial conditions, especially in the context of material processing. In this paper, non-conformities detected during the ultrasonic testing of the steel infrastructure were analysed. The investigation of non-conformity area included the chemical composition analysis, the thermodynamic calculations of the solidification sequence and metallographic analysis. The ultrasonic test results indicated the crocodile effect associated with the thermomechanical processing of steel ingots containing casting defects. This fact was supported by the results of the non-equilibrium solidification sequence. Microstructural analysis of the non-conformity area indicated the presence of non-metallic inclusions and cracks. The crack nucleation and propagation occurred during the thermo-mechanical processing. The microstructure constituents also indicated improperly performed thermo-mechanical processing. The rolling texture and acicular ferrite pointed to improperly performed normalization. The conducted research indicates the need to impose additional requirements on the microstructure of the final product, although it is not required by the EN 10025-2:2019 standard.

Keywords: S355JR *structural steel; Thermo-mechanical processing; Ultrasonic testing; Microstructure; Non-metallic inclusions*

1. Introduction

Despite the steady increase in mega and giga projects worldwide, the civil engineering and construction industry have been lagging behind other sectors such as aerospace, the automotive industry and shipbuilding for more than four decades. Numerous factors contribute to productivity losses in construction projects, with delays and disruptions being the most significant [1]. Although disruptions are calculated in the biding stage, they represent events that interrupt construction program. A delay is described as a scenario in which the completion of the project is postponed due to the client, consultant, supplier or contractor related factors. Delays in construction projects are usually measured by the time taken beyond the originally set date, which is a key factor in evaluating project efficiency [2]. The causes of delays in the construction industry are illustrated on Ishikawa diagram (Figure 1). Depending on whether the fault lies with the contractor or the client, delays can be classified as non-excusable, excusable non-compensable, excusable compensable and concurrent [3]. The environment, finances, labour, management, ownership, project planning and resources represent seven main groups of factors that can lead to delays in construction projects (Figure 1). Overall, the most important factor was found to be design and material challenges, followed by financially based cash flow issues, contractor financial issues and late payments [4]. Although design

and material challenges are categorized as management factors that can affect feasibility studies, material sourcing, scheduling and coordination, they are often associated with inflation and a constant increase in material prices. Therefore, the timely completion of a project is not only affected by budget issues at the project level, but also by the global financial situation [5].

Construction materials constitute a major aspect of building and infrastructure delivery. A habitable square meter of living space could require up to 2.3 tons of hundreds of different types of construction materials [6]. The selection of construction materials is a decisive factor in the engineering and architectural design process. Materials must meet certain requirements to ensure safety, durability and functionality. These criteria include economic factors, mechanical properties, non-mechanical properties, production/construction considerations and aesthetic properties. Even if the material is well suited for a particular application, the availability of the material, the ability to fabricate the material into the desired shape, and the ability to fabricate and erect the structure on site must be considered [7]. The properties and requirements of construction materials are fundamental to the integrity and performance of any building structure. Understanding of these properties and complying with standards and regulations will ensure that materials are selected and used correctly, contributing to the overall success and sustainability of construction projects [8]. The materials required in civil and construction engineering can be classified based on source, composition, sustainability and use. Metallic construction materials are an essential part of modern civil engineering and architecture due to their good strength-to-weight ratio, durability, design versatility and recyclability [9]. Based on their chemical composition, the metallic materials used in construction are divided into ferrous and non-ferrous metals. While ferrous metals refer to iron-based alloys (Fe) with varying carbon content (C), the four most commonly used non-ferrous metals are lead (Pb), zinc (Zn), aluminum (Al) and copper (Cu) [10].
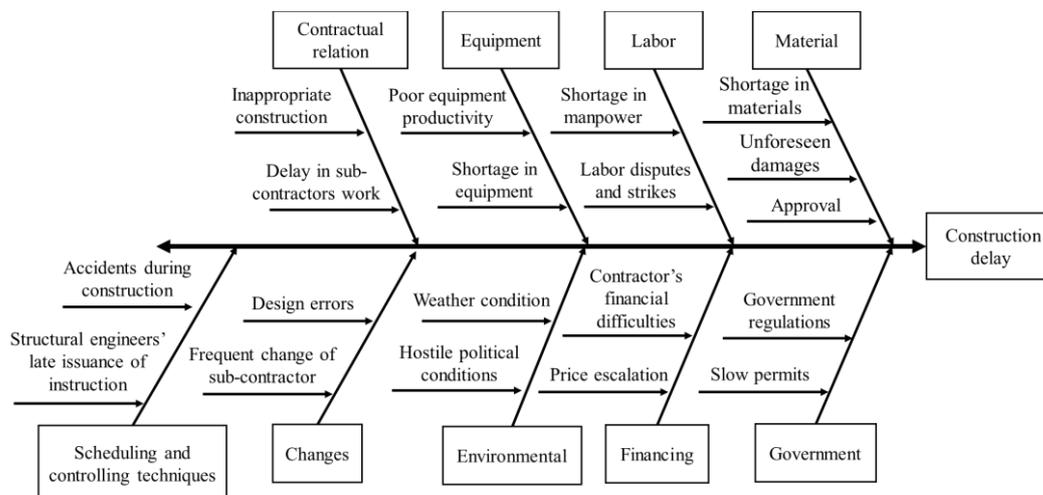
Figure 1. *Ishikawa diagram illustrating delays in construction industry* [1]

The intensive use of steel in civil engineering began in the first quarter of the nineteenth century due to the development of technical solutions to produce standardized steel components on a large scale. The use of steel in architecture and construction allowed flexibility in the shape and size of structures [11].

Based on the general classification, the steels currently available for construction and civil engineering can be divided into four main categories. Most structural steels contain between 0.10 and 0.28 % carbon (C). Steels that contain C as the main alloying element are referred to as structural carbon steels [12]. To improve the strength properties, moderate amounts of one or more alloying elements are added to the carbon structural steels, introducing the subcategories of low-alloy carbon steels [13] and columbium-vanadium-bearing steels. These steels contain less than 2 % of a single alloying element [12]. In older categories of structural carbon steels and high-strength low-alloy steels, mechanical properties were controlled by the hot rolling process. The high-strength properties of

modern carbon steels and alloy steels are obtained by heat treatment. There are two types of heat-treated steels used for construction applications. Similar to carbon structural steels, the strength of heat-treated carbon steel is based on the C content. These types of steels are austenitized, water quenched and tempered between 500 and 700 °C. In addition to C, heat-treated alloy structural steels contain moderate amounts of manganese (Mn), silicon (Si), chromium (Cr) and molybdenum (Mo). Heat treatment of alloy steels involves quenching in oil or water from a minimum of 900 °C and tempering at around 600 °C [14]. The last general category of structural steels includes high nickel (Ni) alloy steels with a low C content. The maraging steels (*martensitic age hardened steel* [15]) are characterized by high strength, high fracture toughness, good weldability and dimensional stability during aging. The low C content reduces the risk of cracking during quenching while the high Ni content and the absence of carbides ensure good corrosion resistance [16].

Despite the difference in chemical composition and heat treatment, the microstructural constituents can be correlated with the general classification of structural steels. Considering the excess C content and the low-temperature hot rolling processing, the microstructure of structural carbon steels is ferrite-pearlite with a uniform grain size. A martensitic microstructure is achieved by quenching in water, resulting in a heat-treated carbon steel with high strength and brittleness. An improvement in toughness and ductility with minimal loss of yield strength is achieved by the precipitation of uniformly distributed carbide particles in the ferrite matrix during tempering [17]. The higher strength of low-alloy steels is the result of alloying with elements (Ni, Mn, Cu) that delay the austenitic transformation and lead to solid solution strengthening of ferrite matrix [18]. The microstructure of heat-treated alloy structural steels is characterized by martensitic transformation and dispersion hardening with Cr, vanadium (V) or Mo containing carbide particles [14]. The precipitation of fine Ni-based particles at dislocation sites improves the properties of maraging steel. These precipitates exhibit different behaviour under mechanical loading compared to the Cr, Mo or V carbides [19].

Since it is possible to correlate the chemical composition, thermomechanical processing and product geometry in the various processing stages with the microstructure and functional properties of the final product, it can be assumed that the materials are the most predictable components in the realization of construction investments [20]. However, it is difficult to ensure the repeatability of quality under industrial conditions, especially in the context of material processing. One of the measures is to examine quality using material, product or production process analysis methods. The stabilization of quality and compliance with requirements is supported by testing. The use of quality instruments, such as quality tools and techniques, enables the continuous identification of non-conformities [21]. Non-conformities are defined as deviations from the desired quality or from specific customer requirements. Non-conformities can relate to procedures or processes, product quality, the occurrence of defects and complaints. The early detection of non-conformities and the development and implementation of corrective actions contribute to the continuous improvement of performance, efficiency, quality and competitiveness [22]. Otherwise, non-conformities are associated with rework or repairs that increase the time and cost of the project [23]. In addition to the negative effects such as loss of profit, loss of market share, damage to reputation and increased turnover in management and staff, rework can also end in litigation [24].

This paper analyses the non-conformities found during the non-destructive testing of the main supporting columns of the steel infrastructure of the compressor station building. Compressor stations are critical facilities within the natural gas infrastructure and active elements of gas transportation networks. Their task is to pressurize natural gas to overcome pressure losses caused by friction, positive slopes and demand nodes. Their partial or complete failure can jeopardize gas transport.

2. Materials and methods

The steel infrastructure of the compressor station building was constructed from non-alloyed structural steel grade S355JR. The plates were manufactured from semi-killed steel and delivered in normalized rolled condition. The inspection certificate was issued in accordance with standard EN 10025-2:2019 *Hot-rolled products of structural steels - Part 2: Technical delivery conditions for non-*

alloy structural steels, which specifies the chemical composition, the dimensions and tolerances of the finished products and the mechanical properties. As the steel infrastructure was joined by welding, additional requirements were placed on the carbon equivalent value (CEV) and ultrasonic testing [25]. The formula of the International Institute of Welding was used to determine the carbon equivalent value (equation 1) [25, 26], while the ultrasonic test was performed according to the procedure for flat products with nominal thickness of more than 6.0 mm [25, 27].

$$CEV = C + \frac{Mn}{6} + \frac{Cr + Mo + V}{5} + \frac{Ni + Cu}{15} \qquad (1)$$

The results listed in the manufacturer's inspection certificate show that the final product complies with the standard and has no non-conformities or defects.

However, as the contractor was obliged to perform an ultrasonic inspection of the weld after completion of the construction work, the results indicated the presence of non-conformities in the base material. To determine the nature of the nonconformance, additional characterization of the chemical composition and microstructure of the plated was performed. Sampling for additional tests is shown in Figure 2.
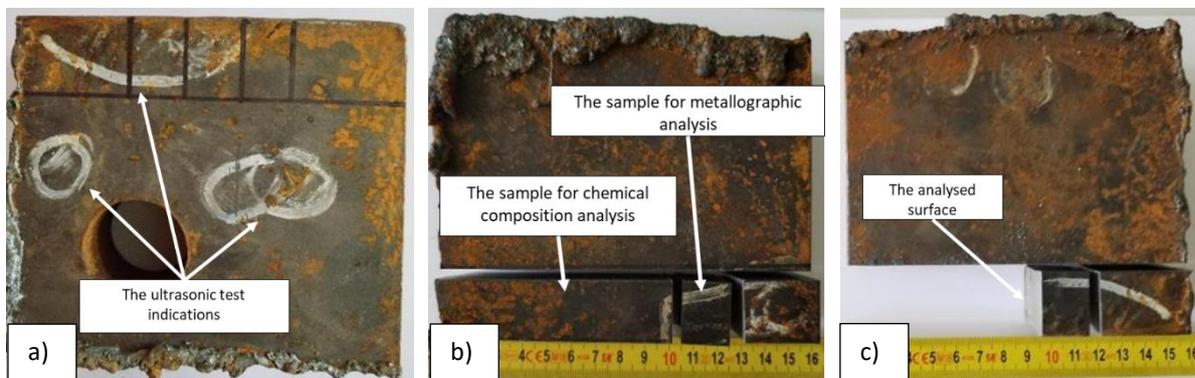
Figure 2. *The sampling for additional tests: a) the ultrasonic test indications, b) chemical composition and metallographic analysis, c) the indicated surface for microstructural analysis*

The sampling for the chemical composition and the metallographic analysis was based on the results of the ultrasonic testing. To determine the nature and cause of the non-conformities, samples for metallographic analysis were taken from the previously marked locations (Figure 2 a). To avoid the possible influence of flame cutting on the microstructure development, the samples were taken further away from the edge of the plate (Figure 2 b). The metallographic analysis was performed on the surface perpendicular to the rolling direction (Figure 2 c).

The chemical composition of the samples was analysed using a LECO GDS 900 Glow Discharge Atomic Emission Spectrometer equipped with the Cornerstone software package. Prior to analysis, the instrument was conditioned with a standard sample. During conditioning, the chemical composition of the standard sample was measured five times and compared with the database. After a suitable match was achieved, the test method was selected. A sample of S355JR steel was tested using the low-alloy steel method. The chemical composition was measured on the surface perpendicular to the rolling direction. The measurement was repeated three times.

The results of the chemical composition analysis were used as input parameter for the calculation of the equilibrium and non-equilibrium solidification sequence using Thermo-Calc 2022 a software support. The calculations were performed using the TCFE12: Steel/Fe-Alloys v12.0 database for iron and steel. The equilibrium solidification sequence was calculated for 1.0 g of melt at a pressure of 1 x 10^5 MPa and the amounts of Fe, C, Mn, Si, sulphur (S) and phosphorus (P). The calculation was performed in a temperature range from 1600 to 25 °C. For the calculation of the Scheil non-equilibrium solidification sequence a cooling rate of 0.71 m/s was specified additionally.

The samples for the metallographic analysis were prepared using standard grinding and polishing techniques. The macrostructure and microstructure of the samples were analysed in polished and etched condition. The samples were etched in the 2 % NITAL solution (2 % solution of nitric acid in alcohol). The light microscopy at lower magnifications was performed using Olympus SZ11 stereo microscope, while higher magnification observations were obtained using Olympus GX51 inverted metallographic microscope equipped with Stream Motion software support.

3. Results and discussion

The results of the ultrasonic tests performed after welding with the corresponding parameter tables can be found in Figure 3.
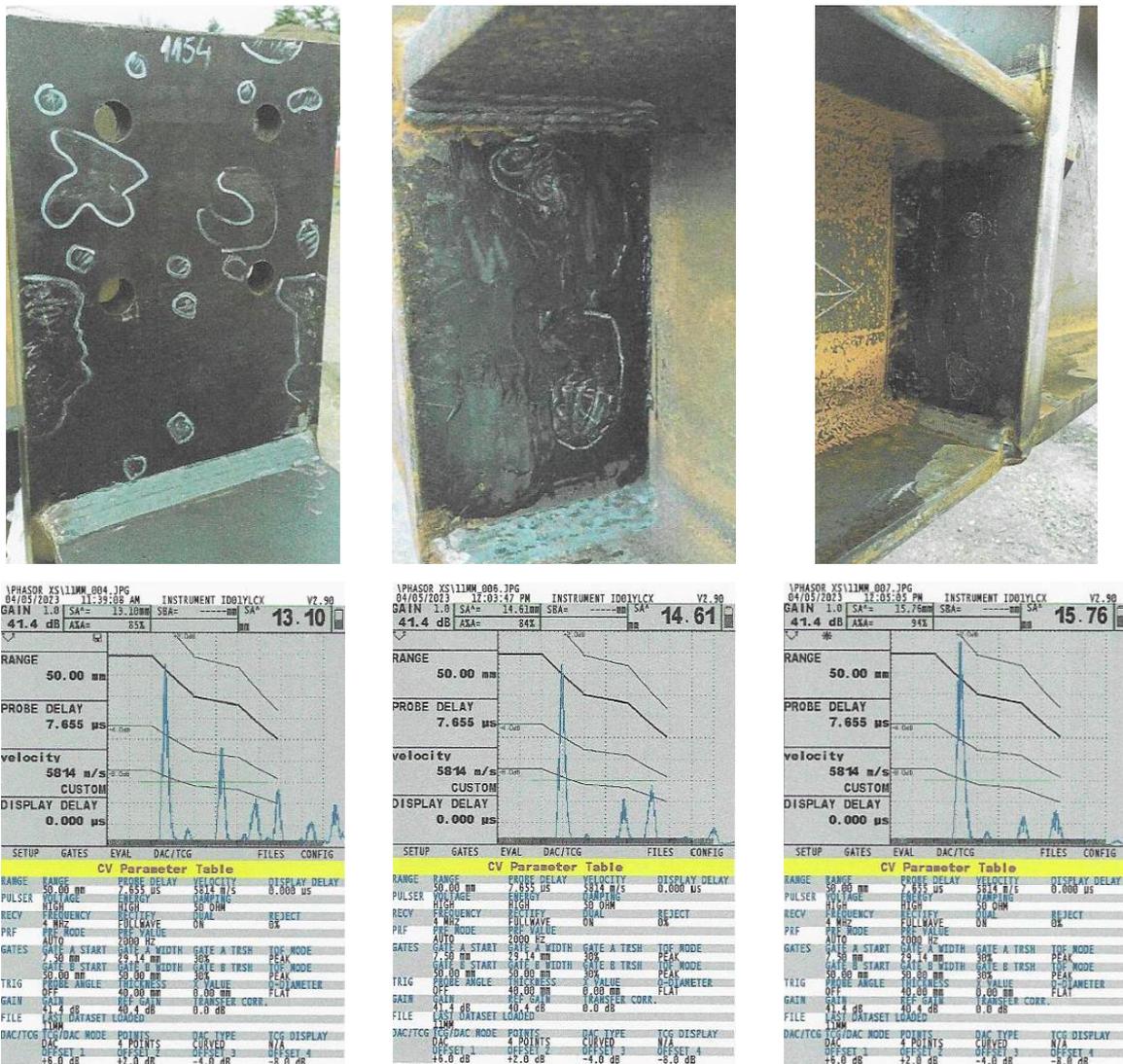
Figure 3. *The results of ultrasonic tests*

At a depth of 20 mm, the signs of the crocodile effect appear on the entire surface of the base material (Figure 3). The intensity of the crocodile effect signal is usually 50 % of the allowable limit, although the limit is occasionally exceeded. Other layered signals appear at different depths from 10 to 30 mm. The deviations in the signal were not detected in the welds. The appearance of the crocodile effect in steels is usually the result of thermomechanical processing of ingots, in which segregation of alloying elements and casting defects have occurred.

The chemical composition of the steel S355JR is within the limits specified in the standard EN 10025-2:2019 for the final product analysis (Table 1). The Mn content (1.48 wt.%) and a CEV within the limits

ensure good weldability of the base metal. The appearance of hot cracks in weld and heat affected zone is not expected. However, a CEV of 0.42 indicates the need to preheat the base material before welding.

Table 1. *The chemical composition of the plate*

	Composition, wt.%						Carbon equivalent value, CEV
Sample	C	Si	Mn	P	S	Cu	
S335JR plate	0.165	0.21	1.48	0.015	0.004	0.01	0.42
EN 10025-2:2019 [25]	< 0.21	< 0.60	< 1.70	< 0.045	< 0.045	< 0.60	0.47+0.01[*]

[*]Based on the Si content (Si < 0.25 wt.%) the increase in CEV by 0.01 is permissible

The equilibrium and non-equilibrium phase diagrams are illustrated in Figure 4 a and b with corresponding reactions given in Tables 2 and 3.
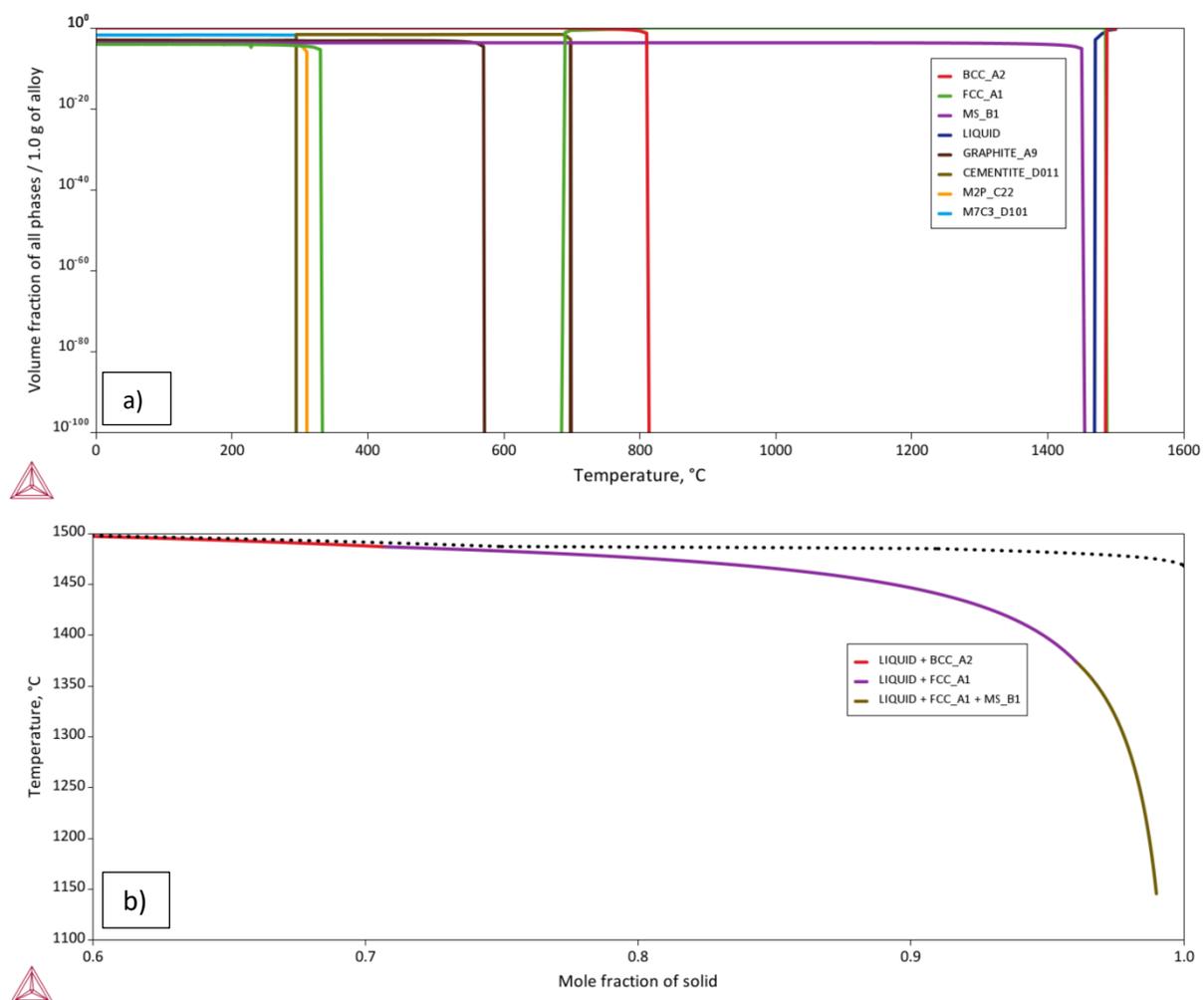
Figure 4. *The results of Thermo-Calc calculations: a) equilibrium, b) non-equilibrium*

The microstructural evolution under equilibrium conditions starts with the solidification of delta iron (δ-Fe) (Table 2, reaction no. 1), followed by the solidification of austenite (γ-Fe) (Table 2, reaction no. 2) and non-metallic high-temperature inclusions of the MnS type (Table 2, reaction no. 3). The development of the ferritic microstructure continues in the temperature range between 810.9 and 684 °C (Table 2, reaction no. 4), when the parallel solidification of cementite (Fe₃C) begins and leads

to the formation of pearlite (α-Fe + Fe₃C) (Table 2, reaction no. 5). The equilibrium solidification ends with the precipitation of carbide particles of the type Mn_7C_3 (Table 2, reaction no. 6).

In contrast to equilibrium solidification, the non-equilibrium solidification sequence takes place in the narrower temperature interval between 1514 °C and 1376.6 °C. The non-equilibrium solidification sequence recognizes the solidification of delta iron (δ-Fe), austenite (γ-Fe) and non-metallic MnS inclusions (Table 3). More importantly, the Scheil diagram shows a wide range between equilibrium and non-equilibrium solidification, indicating the possibility of segregation and the occurrence of casting defects during solidification.

Table 2. The equilibrium solidification sequence according to the Thermo-Calc calculations

Reaction No.	Reaction	Temperature, °C
1.	Liquid (L) → BCC_A2 (delta iron (δ-Fe))	1510
2.	Liquid (L) + BCC_A2 (delta iron (δ-Fe))→ FCC_A1 (Austenite (γ-Fe))	1488.1
3.	Liquid (L) → FCC_A1 (Austenite (γ-Fe)) + MS_B1 (MnS)	1450
4.	FCC_A1 (Austenite (γ-Fe)) → BCC_A2 (Ferrite (α-Fe))	810.9
5.	FCC_A1 (Austenite (γ-Fe)) + BCC_A2 (Ferrite (α-Fe)) → BCC_A2 (Ferrite (α-Fe)) + CEMENTITE_D011 (Cementite (Fe₃C))	684
6.	BCC_A2 (Ferrite (α-Fe)) + CEMENTITE_D011 (Cementite (Fe₃C)) → BCC_A2 (Ferrite (α-Fe)) + M7C3_D101 (Mn₇C₃)	294

Table 3. The non-equilibrium solidification sequence according to the Thermo-Calc calculations

Reaction No.	Reaction	Temperature, °C
1.	Liquid (L) + BCC_A2 (delta Fe (δ-Fe))	1514
2.	Liquid (L) + FCC_A1 (Austenite (γ-Fe))	1487
3.	Liquid (L) + FCC_A1 (Austenite (γ-Fe)) + MS_B1 (MnS)	1376.6

The macrostructure of the samples in etched condition at the magnification of 17.5 X is shown in Figure 5.
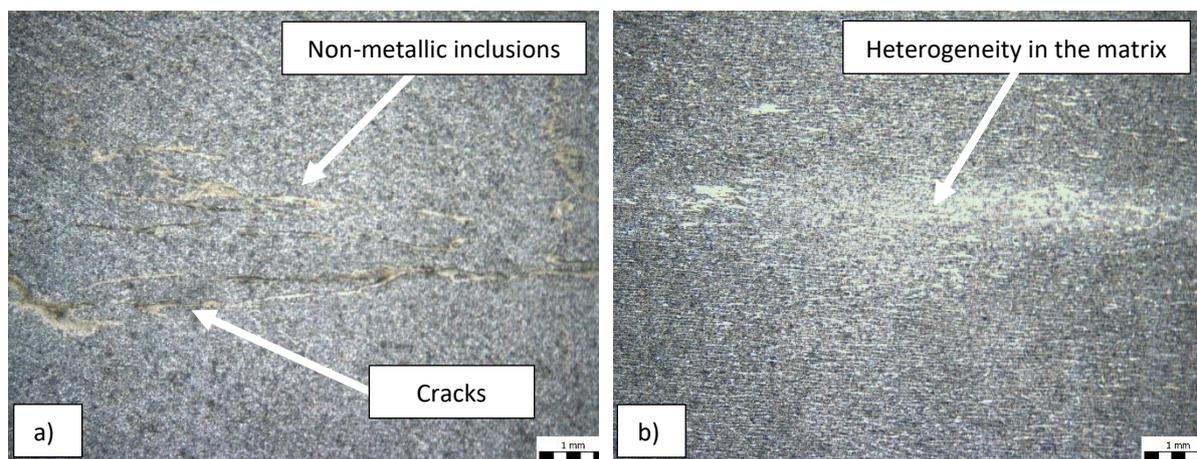
Figure 5. The macrostructure of the sample in etched condition at the magnification of 17.5 X: a) cracks and non-metallic inclusions, b) heterogeneity in the matrix

After standard metallographic preparation and etching, deviations in the analysed surface were observed at the depth of 14 and 20 mm (half of the cross-section of the plate). The results of the macrostructural analysis of the observed surface indicate the presence of non-metallic inclusions, cracks (Figure 5 a) and heterogeneities in the matrix structure (Figure 5 b). Figure 6 shows the microstructure of the sample in the polished and etched condition at different magnifications.
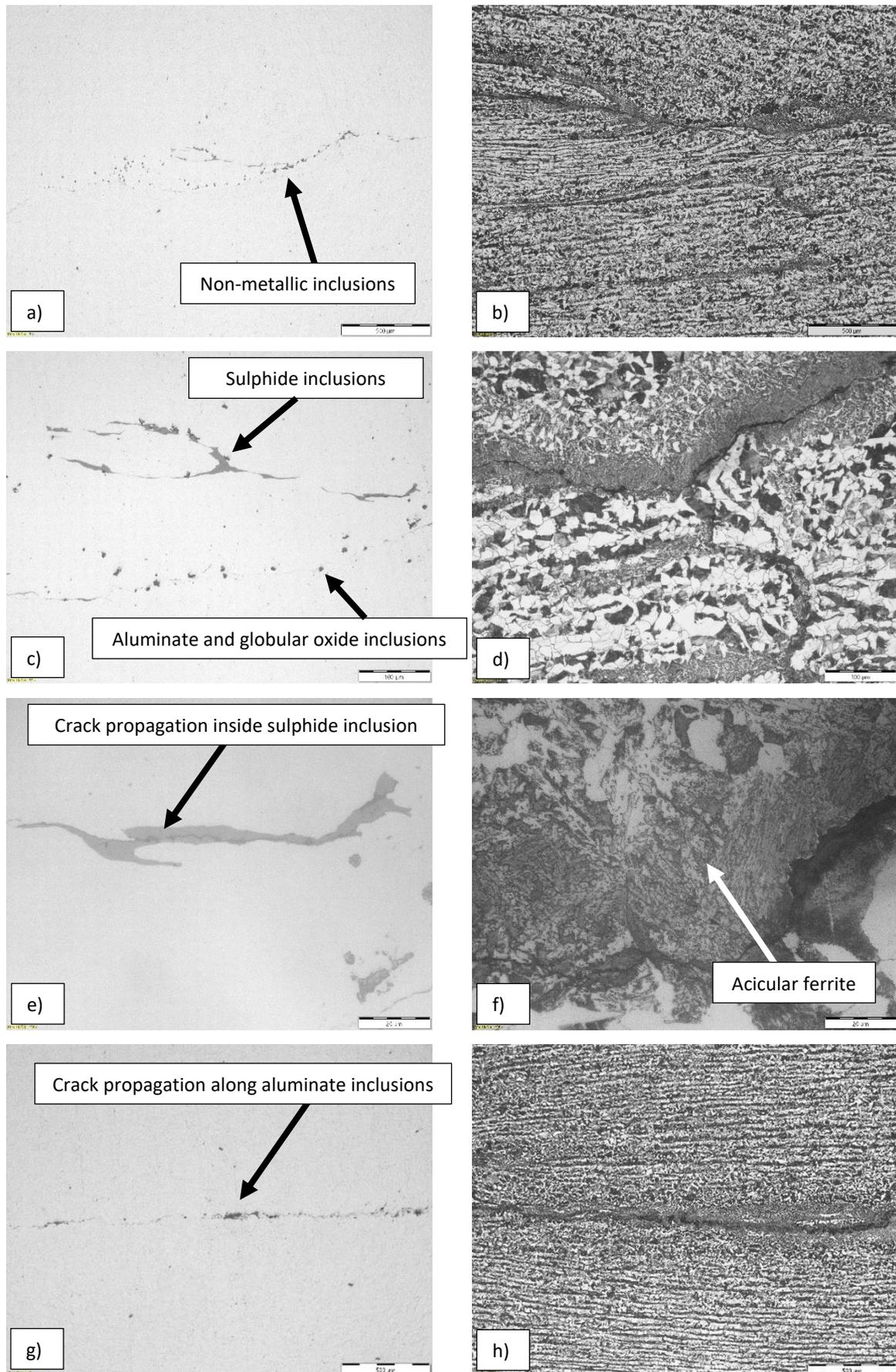
Figure 6. The microstructure of the sample in the polished and etched condition at different magnifications

Non-metallic inclusions of the sulphide type (Figure 6 a), aluminate and globular oxide type (Figure 6 c) as well as cracks (Figure 6 e) can be observed in the microstructure of the non-conformity area in the polished condition. Although it is not possible to clearly determine the location of crack initiation due to the sampling method, the propagation (advancement) of the cracks includes the non-metallic inclusions (Figure 6). Since sulphide inclusions have a lower hardness compared to the matrix, the crack appears inside the inclusion (Figure 6 d). On the other hand, aluminate and globular oxide inclusions have a higher hardness compared to the matrix, which is why crack propagation occurs along the inclusion/matrix interface (Figure 6 g).

The microstructure of the matrix is ferrite-pearlite with a pronounced rolling texture (Figure 6). As the steel was supplied in a normalized rolled condition, the presence of the rolling texture is not expected. In the area of non-conformity there is a deviation in the rolling texture orientation (Figure 6 b and d) and the appearance of mixed morphology ferrite (Figure 6 d and f). The ferrite has an acicular needle-like morphology (Figure 6 d and f). The presence of acicular ferrite indicates that normalization was performed at temperatures above the AC_3 line and an austenitic microstructure was achieved. The acicular ferrite nucleates heterogeneously on non-metallic inclusions within the austenitic grains. Higher magnification images indicate crack propagation along the sulphide and oxide inclusions during thermo-mechanical processing (Figure 7).

Crack propagation along inclusions
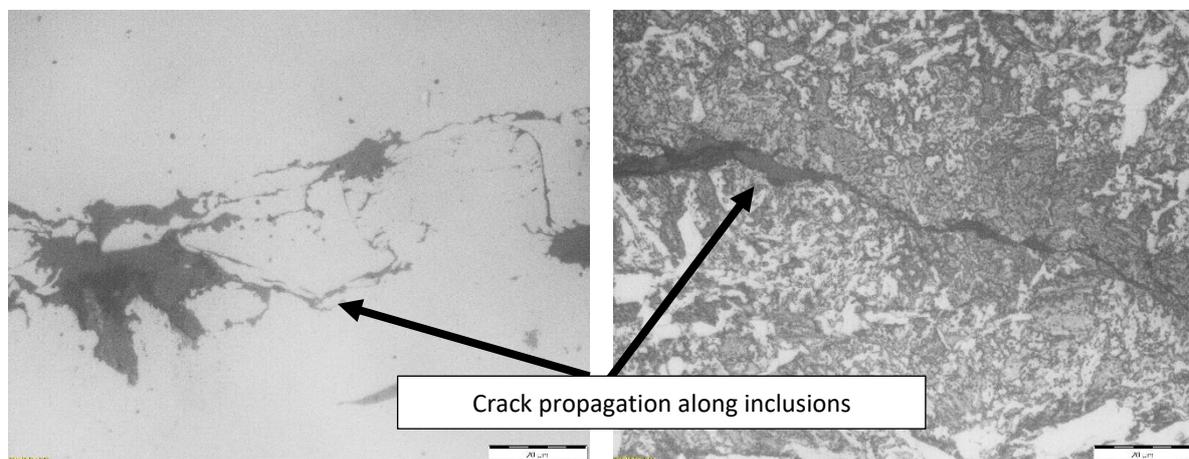
Figure 7. *Involvement of non-metallic inclusions in crack propagation: a) polished, b) etched condition*

4. Conclusions

The study investigated the non-conformities in S355JR steel plates used for the construction of the compressor station building infrastructure. Although the inspection certificate issued in accordance with the EN 10025-2:2019 standard did not indicate any deviations in the chemical composition, dimensions or mechanical properties of the finished product, the ultrasonic testing carried out after completion of the construction work indicated the presence of non-conformities in the base material. The evaluation of the recorded parameters and the intensity of the ultrasonic signal indicated the appearance of the crocodile effect at depths of 10, 20 and 30 mm. The crocodile effect is a non-conformity that usually occurs during the thermo-mechanical processing of ingots that contain casting defects and segregations. The occurrence of casting defects, segregations and non-metallic inclusions of the sulphide MnS type during the solidification of the ingots was also supported by the results of the non-equilibrium solidification sequence. Microstructural analysis of the non-conformity area in polished condition indicated the presence of non-metallic inclusions of sulphide, aluminate and globular oxide type as well as cracking. Due to the difference in hardness between the non-metallic inclusions and the matrix, the cracks propagated through the sulphide inclusions and the inclusion/matrix interface. The matrix of the non-conformity area is ferritic-pearlitic with the appearance of rolling texture and acicular ferrite. Since the material was delivered in normalized rolled condition, the complete removal of the rolling texture was expected due to the mechanisms of recrystallization and

grain growth. Instead, localized heterogeneous nucleation of acicular ferrite occurred. Crack propagation occurred along the sulphide and oxide inclusions during thermo-mechanical processing. Although not defined in the standard, it was finally recommended to establish additional requirements for thermo-mechanical processing to control the microstructure of the final product, focussing on the type and content of non-metallic inclusions and the final allotropic modification and morphology of the solid solution of the iron matrix.

Acknowledgments

References

[1] Sanni-Anibire, O.M., Zin, M.R., Olatunji, O.S., 2022. Causes of delay in the global construction industry: a meta analytical review. Int. J. Constr. Manag. 22, 1395–1407.

[2] Abo El-Wafa, M.M., Mosly, I., 2024. An extensive examination of the barriers faced by contractors leading to project delays. Glob. J. Eng. Technol. Adv. 18, 152–167.

[3] Kikwasi, G., 2013. Causes and Effects of Delays and Disruptions in Construction Projects in Tanzania. Australas. J. Constr. Econ. Build. 1, 52-59.

[4] Kazaz, A., Ulubeyli, S., Tuncbilekli, N.A., 2012. Causes of delays in construction projects in Turkey. J. Civ. Eng. Manag.18, 426–435.

[5] Musarat, M.A., Alaloul, W.S., Liew, M.S., Maqsoom, A., Qureshi, A.H., 2020. Investigating the impact of inflation on building materials prices in construction industry. J. Build. Eng. 32, 101485.

[6] Akadiri, P.O., Chinyio, E.A., Olomolaiye, P.O., 2012. Design of a sustainable building: A conceptual framework for implementing sustainability in the building sector. Buildings. 2, 126–152.

[7] Al-Nuaimi, S., Banawi, A.A.A., Al-Ghamdi, S.G., 2019. Environmental and economic life cycle analysis of primary construction materials sourcing under geopolitical uncertainties: A case study of Qatar. Sustain. 11, 2-26.

[8] Mamlouk, M.S., Zaniewski, P.J., 2018. Materials for civil and construction engineers, Pearson Education Limited 2018, Essex.

[9] Findik, F., Findik, F., 2021. Civil engineering materials. Herit. Sustain. Dev. 3, 154–172.

[10] Claisse, P.A., 2015. Alloys and Non-Ferrous Metals. Civ. Eng. Mater. 32, 361–367.

[11] Gonçalves, M.C., Fernanda, M.F., 2015. Materials for construction and civil engineering: Science, processing, and design. Springer Cham.

[12] Grider, A., Ramirez, J.A., Yun, J.M., 2003. The Civil Engineering Handbook, CRC Press.

[13] Xie, Z., Shang, C., Wang, X., Wang, X., Han, G., Misra, R., 2020. Recent progress in third-generation low alloy steels developed under M3 microstructure control. Int. J. Miner. Metall. Mater. 27, 1–9.

[14] Brantley, R.T., Brantley, L.R., Aterials, M., 2004. Construction Materials. Educational Low-Priced Book Scheme (ELBS) Longman.

[15] Flint, G.N., Oldfield, J.W., Dautovich, D.P., Mahi, F.T., 2017. Corrosion of Iron–Nickel Alloys and Maraging Steel. Elsevier.

[16] Rajan, T.V., Sharman, C.P., 2023. Heat treatment Primciples and Techinques. PHI.

[17] Shibata, A., Miyamoto, G., Morito, S., Nakamura, A., Moronaga, T., Kitano, H., Gutierrez-Urrutia, I., Hara, T., Tsuzaki, K., 2023. Substructure and crystallography of lath martensite in as-quenched interstitial-free steel and low-carbon steel. Acta Mater. 246, 118675.

[18] Tan, X., Lu, W., Rao, X., 2022. Effect of ultra-fast heating on microstructure and mechanical properties of cold-rolled low-carbon low-alloy Q&P steels with different austenitizing temperature. Mater. Charact. 191, 112086.

[19] Albu, M., Panzirsch, B., Schröttner, H., Mitsche, S., Reichmann, K., Poletti, M.C., Kothleitner, G., 2021. High-resolution microstructure characterization of additively manufactured x5crnicunb17-4 maraging steel during ex and in situ thermal treatment. Materials (Basel). 14, 7784.

[20] Czajkowska, A., 2015. Identification and analysis of non-conformities in production of construction materials with the example of hot- rolled sheet metal. METAL 2015, Brno.

[21] Siwiec, D., Pacana, J., Pacana, A., 2023. A Novelty Procedure to Identify Critical Causes of Materials Incompatibility. Materials (Basel). 16.

[22] Knop, K., 2022. Multivariate Nonconformity Analysis for Paving Stone Manufacturing Process Improvement. Manag. Syst. Prod. Eng. 30, 331–341.

[23] Ulewicz, R., Czerwińska, K., Pacana, A., 2023. A Rank Model of Casting Non-Conformity Detection Methods in the Context of Industry 4.0. Materials (Basel). 16.

[24] Alrasheed, K.A., Soliman, E., Al Mesbah, F.E., 2023. Dispute Classification in Construction Projects Based on Litigation Cases. J. Leg. Aff. Disput. Resolut. Eng. Constr. 15, 1–9.

[25] EN 10025-2:2019 Hot rolled products of structural steels - Part 2: Technical delivery conditions for non-alloy structural steels, European Standard.

[26] Alhassan, M., Bashiru, Y., 2021. Carbon equivalent fundamentals in evaluating the weldability of microalloy and low alloy steels. World J. Eng. Technol. 9, 782-792.

[27] EN 10160 Ultrasonic testing of steel flat product of thickness equal or greater than 6 mm (reflection method), European Standard.